SCIENCE CHINA
Technological Sciences

Investigation of electrons inside the satellite by the Geant4 simulation

LI XiaoCan, CHEN HongFei, HAO YongQiang, ZOU Hong and SHI WeiHong

Citation: SCIENCE CHINA Technological Sciences **54**, 2271 (2011); doi: 10.1007/s11431-011-4521-y

View online: http://engine.scichina.com/doi/10.1007/s11431-011-4521-y

View Table of Contents: http://engine.scichina.com/publisher/scp/journal/SCTS/54/9

Published by the Science China Press

SCIENCE CHINA
Technological Sciences

SCIENCE CHINA
Technological Sciences

September 2011 Vol.54 No.9: 2271–2275
doi: 10.1007/s11431-011-4521-y

Investigation of electrons inside the satellite by the Geant4 simulation

LI XiaoCan, CHEN HongFei*, HAO YongQiang, ZOU Hong & SHI WeiHong

Institute of Space Physics and Applied Technology, School of Earth and Space Sciences, Peking University, Beijing 100871, China

Received January 30, 2011; accepted June 13, 2011; published online July 22, 2011

The measurement of the electron radiation inside the satellite is important for engineering and space environment researches. The particle radiation detectors (PRD) on board CBERS-1 and CBERS-2 made great contribution to understanding of the space environment. Then, what is the radiation relationship between inside and outside the satellite? The Monte Carlo simulation with Geant4 was implemented to study the problem. The boundaries of the energy bins of 0.5 and 2 MeV were precisely corresponding to outside energies of 0.99 and 2.52 MeV, respectively. Besides the changes of the energy bins, the fluxes inside were smaller than those of the corresponding bins outside. The spectrum inside the satellite was harder than that outside. An indicator was that the flux ratio of the high energy bin to the low energy bin increased more than 20% from outside to inside. The geometric factor (GF) relates to the incident energy of electrons. By using the AE-8 model to derive the incident spectrum, the GFs of the low and high energy bins were 1.15 and 0.70 cm^2 sr, respectively. GF of the low energy bin was larger than that of the high energy bin. But they were both smaller than the previous results. It was due to the scattering, straggle and shielding effects.

electron radiation in satellite, electron detector, Monte Carlo simulation, Geant4

Citation: Li X C, Chen H F, Hao Y Q, et al. Investigation of electrons inside the satellite by the Geant4 simulation. Sci China Tech Sci, 2011, 54: 2271–2275, doi: 10.1007/s11431-011-4521-y

1 Introduction

The objective of the particle radiation detector (PRD) developed by Peking University was to measure the particle radiation inside the satellite [1]. It has been onboard the ZY-1 satellites (CBERS-1 and CBERS-2). The measurement of PRD is important for the anti-radiation design of space engineering and for the research of space physics, too [2–7]. The data of the PRD showed that the electron radiation inside the satellite is related to the electron radiation outside. The spectrum is relatively harder than the radiation outside the satellite [8].

The electron sensing head of the PRD is of a two-layer structure. The first layer is a thin and completely depleted detector, namely ΔE layer, to identify the electrons. The second layer is a thick Si-Li draft detector to measure the energy of the electrons. The PRD has two energy bins that are the low energy bin (0.5 MeV$\leqslant E \leqslant$2.0 MeV) and high energy bin (E>2.0 MeV). Chen et al. used the range concept of electrons to predict the geometric factor (GF) [9]. They found that the GFs of the two bins may be undervalued before and the GF of the low energy bin is larger than that of the high energy bin. In their works, the scatting and straggle effects of electrons were not considered. However, these effects can cause the range of electrons in matter ambiguous by probabilities.

The calibration of the PRD was implemented by the experiments with β and γ radiation sources. The two energy boundaries of 0.5 and 2.0 MeV were determined by the cali-

*Corresponding author (email: hfchen@pku.edu.cn)

bration. Besides the calibration, more comprehensive studies of the detector, including the effects of the satellite skin, is necessary in order to enhance the researches of the radiation environment of the satellite, such as the directional responses and the effects of the satellite skin.

The satellite skin that may shield the electrons was treated as 2 mm equivalent aluminum [6]. Due to some energy lost in the skin, the energy bins (0.5–2 MeV and >2 MeV) of PRD inside the satellite are equivalent to energy bins of 1.49–2.96 MeV and >2.96 MeV outside, respectively. Zou et al. pointed out that the peak integral flux of 0.5–2.0 MeV inside the satellite was smaller than the peak integral flux of 1.49–2.96 MeV outside by the AE-8 model [6].

The real skin of the satellite is of the honeycomb structure. In our previous work [10], the honeycomb skin was equivalent to 1 mm aluminum rather that 2 mm by the Monte Carlo simulation. The differences between the honeycomb skin and the 1 mm Al skin are smaller than 10% in most cases in the aspects of energy loss of electrons, shielding effects and secondary electrons producing. Since the differences between 2 millimeter aluminum and satellite skin are much larger (more than 60% for 2 MeV electrons) by the Monte Carlo simulation, there were errors in Zou's results [6]. It was not mentioned in Zou's paper that how the skin was equivalent to 2 mm Al, but they did not use the Monte Carlo simulation. In this paper, we corrected the errors following the Monte Carlo simulation.

In this article, Geant4, a kind of the Monte Carlo toolkit, was used to investigate the measurements of electrons inside the satellite and the effects of the satellite skin. Geant4 was developed by the European Organization for Nuclear Research (CERN) for simulating the passage of particles through matter [11]. It includes a complete range of functionality such as tracking, geometry, physics models and hits. It has been widely used in the high energy physics, nuclear physics, medical research and space science research [12].

Monte Carlo methods have advantages that traditional numerical methods don't have [13, 14]. Firstly, Monte Carlo methods are suitable to treat complex problems, such as systems with complex geometries and coupled degrees of freedom. Since traditional methods have to make several assumptions in these cases, the accuracy of the results can't be guaranteed. Secondly, Monte Carlo methods are most suited to simulate systems with significant uncertainty, because they are of stochastic simulation methods. And there are several kinds of stochastic processes in nature, such as radioactive decay and transportation process of particles in the matter. Finally, Monte Carlo methods can give all kinds of information of particles in the matter, which is impossible for a single traditional numerical method.

The behavior of electrons in the PRD is essentially a transportation process of electrons in the matter. Considering its complex geometry, complex physics processes, strong scatting effects and secondary electrons production, Geant4 is helpful to analyze the electron detector of the PRD and the skin effects for the radiation inside the satellite.

2 Corresponding energy bins outside

Since the satellite skin can be treated as 1 mm equivalent aluminum which is much simpler and better in the simulation, the work in this paper treats the satellite skin as a 1 mm equivalent aluminum plate. This 1 mm Al plate separates the geometry into two sides. One is inside the satellite while the other is outside. All high energy electrons in the satellite are coming from the outside.

A series of monoenergetic electrons were input to the simulation process in order to get their residual energy after passing through 1 mm aluminum plate. The energy at count peak was chosen as the characteristic energy corresponding to the incident energy. Figure 1 shows the residual energy spectrum of 3 MeV incident electrons with the normal incident angle. The circle in Figure 1 indicates the count peak. The energy of it is called the peak position, marked as E_p. E_p is 2.65 MeV for 3 MeV energy electrons that have incidence at the normal direction. The shadow area of Figure 1 is the total count of the peak C_p. The other counts out of the shadow area are treated as noises.

Considering the arbitrary incidence, E_p decreases with the increase of the incident angle because electrons with oblique incidence may have to pass thicker aluminum. The solid angle for incident angle θ with the range $d\theta$ is equal to $2\pi\sin\theta d\theta$. Assuming that the simulation electrons are isotropic. The counts for incident angle θ with the range $d\theta$ is equal to

$$dC = \frac{N_0}{4\pi}\frac{C_p(\theta)}{100000}2\pi\sin\theta d\theta, \quad (1)$$

where N_0 is the number of omnidirectional electrons.

Figure 2 shows the simulation for all incident angle. The dashed-line indicates the peak positions for different incidences while the solid line indicates $C_p(\theta)2\pi\sin\theta$. The latter has a peak at 50° that is defined as the most sensitive incident angle. The peak position E_p at this angle is chosen as

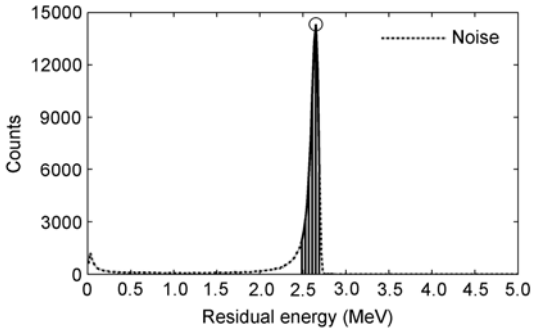

Figure 1 Residual energy spectrum of 3 MeV incident energy for electrons.

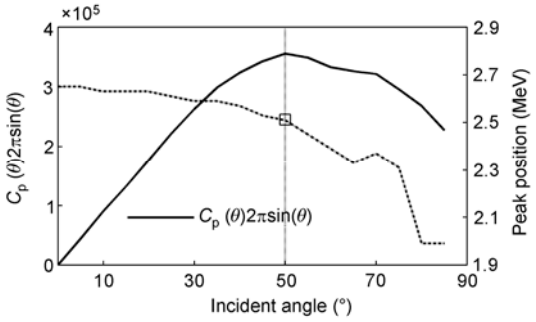

Figure 2 Simulation of 3 MeV electrons for different incidences.

the residual energy of 3 MeV electrons that pass the aluminum plate from the arbitrary incidence.

Similarly, the peak positions for other incident energies with arbitrary incidences from outside of the satellite were obtained, such as for 0.5, 0.7, 0.9, 1, 1.5, 2, 2.5, 3, 3.5, and 4 MeV. The incident energies 0.99 and 2.52 MeV of the outside were corresponding to residual energies 0.5 and 2 MeV inside, respectively, which are the energy boundaries of the PRD located inside the satellite. They are lower than the results of Zou et al. [6], i.e., 1.49 and 2.96 MeV, because the equivalent thickness of the skin was 1 mm rather than 2 mm [10].

3 Smaller flux inside

The energy bins of 0.5–2 MeV and >2 MeV inside were equal to 0.99–2.52 MeV and >2.52 MeV outside as discussed in section 2. What is the relation of their fluxes?

As one result of Zou et al. [6], the measurement of the low energy bin of PRD is smaller than that predicted by the AE-8 model. Since the function of the electron spectrum in the space roughly decreases exponential as energy increases, the electron flux inside the satellite predicted with the AE-8 model is undervalued more if the boundaries of 1.49 and 2.96 MeV change to 0.99 and 2.52 MeV. It implies that the measurement of the low energy bin of PRD is much smaller than the prediction by the AE-8 model.

The radiation inside the satellite is affected by the skin. These effects are related to the energy of electrons. Assuming the integral flux spectrum in the space is of the exponential function, one can have

$$F(E) = F(>2\,\text{MeV})\exp\left[(2-E)/E_0\right], \qquad (2)$$

where E_0 is a factor to indicate the hardness of the spectrum. The larger E_0, the harder the spectrum. For convenience, $F(E)$, instead of $F(>E)$, represents the integral flux of electrons of the energy greater than E; $1/E_0$, instead of E_0, determines the spectrum hardness. $1/E_0$ is close to zero if the spectrum is very hard. Really, the >10 MeV electrons are rare in earth's magnetosphere. The simulation results of $1/E_0 \leqslant 0.5$ MeV^{-1} may be unpractical. On the other side, if $1/E_0$ is larger than 4 MeV^{-1}, the proportion of electrons with high energy is very small. It is also unpractical.

Yan et al. gave a set of equations to express the $1/E_0$'s relation with the solar cycle and L value. It shows that $1/E_0$ increases with L value and $1/E_0$ is periodic in a solar cycle [15]. This is consistent with the FLUMIC model [16]. By combining the result of Yan et al. and the FLUMIC model, $1/E_0$ can be derived to be between 1.41 and 4.00 MeV^{-1} in the outer radiation belt (3–7 R_E) in most cases. In addition, Ryden et al. found that the repeated hardening and softening of the spectrum is well correlated with the enhancement events of electrons in the medium Earth obit (MEO), and that $1/E_0$ can be 0.5 MeV^{-1} in some cases [17]. Therefore, the value of $1/E_0$ in the outer radiation belt can be chosen as 0.5–4 MeV^{-1}, which covers GEO and MEO. However, the value of $1/E_0$ in the low Earth orbit (LEO) is not so clear to us because the condition is more complicated with the South Atlantic Anomaly (SAA) and the polar region. The AE-8 model may be a choice for LEO. $1/E_0$ can be roughly estimated for the CBERS orbit by the AE-8 model. The result is about 1.43 MeV^{-1}. Anyway, setting $1/E_0$ from 0.5 to 4 MeV^{-1} can cover most cases in the earth's radiation belts.

Figure 3 shows the ratios of the fluxes inside to outside for the two energy bins. It is obvious that the fluxes inside are smaller than the corresponding fluxes outside. It may be caused by the electron shielding effects of the satellite skin, which are different of electrons with different energy.

4 Harder spectrum inside

Figure 4 explains the fluxes change from outside to inside. The subscripts o and i represent the fluxes outside and inside the satellite, respectively. The vertical axis is exponential, so the exponential functions of the integral flux spectra according to eq. (2) are straight lines with a negative slope. The smaller the slope, the harder the energy spectrum. The flux of the low energy bin inside is equal to $F_i(0.5)$–$F_i(2)$ while the flux of it outside is $F_o(0.99)$–$F_o(2.52)$.

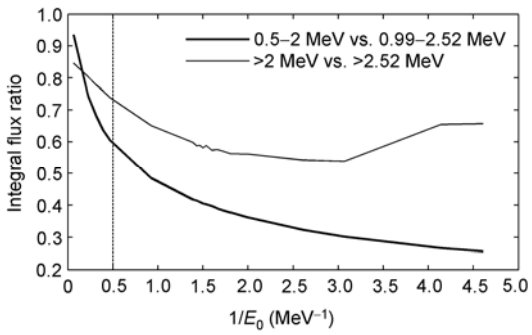

Figure 3 Ratio of inside flux to outside flux.

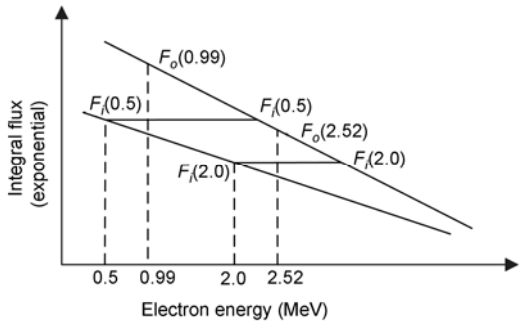

Figure 4 The functions of the electron spectra inside and outside.

It is obvious that $F_i(0.5)$ and $F_i(2)$ are smaller than $F_o(0.99)$ and $F_o(2.52)$, respectively because of the scatting and straggle of electrons. The simulation shows that $F_i(0.5)$–$F_i(2)$ is smaller than $F_o(0.99)$–$F_o(2.52)$. It implies that $F_o(2.52)$–$F_i(2)$ is smaller than $F_o(0.99)$–$F_i(0.5)$. If the slope of the line of the spectrum inside is equivalent to or larger than the slope outside, there is no such conclusion. So the slope of the line of the spectrum inside in Figure 4 is less than that outside. It means the spectrum inside is harder than outside.

The ratio of the flux of the high energy bin to the low energy bin ($R_{\rm hl}$) is also a symbol to indicate the hardness of the spectrum. The larger $R_{\rm hl}$ is, the harder the spectrum will be. Figure 5 gives the ratios both inside and outside of the satellite. It is obvious that the ratio inside is larger than the ratio outside the satellite. Their difference is about 20% when $1/E_0$ is 0.5 $\rm MeV^{-1}$. And it is about 70% when $1/E_0$ is 3 $\rm MeV^{-1}$. Therefore, the electron flux spectrum inside is harder than the flux spectrum outside after passing through the satellite skin.

5 Geometric factor

Chen et al. suggested that the geometric factor of the electron measurement was related to the energy incidence [9]. In this paper, the model of the head with shielding effects considered was precisely constructed from the mechanical scheme and the materials. The satellite skin is not considered if one just discusses the GF of the head.

Firstly, the monoenergetic electrons of 0.5 and 2 MeV were used in the simulation to get the residual energy in the second detector (*E* detector) of the head like we did in section 2. They were 0.46 and 1.98 MeV, respectively. These two values were used as the discrimination levels, say S_1 and S_2, for the low (0.5–2 MeV) and high (>2 MeV) energy bins.

Secondly, the simulation used the AE-8 model to predict the spectrum incidence. Figure 6 shows the differential and integral fluxes of the AE-8 model on solar maximum by SPENVIS [18], which were averaged over the orbit of the ZY-1 satellite.

The head of the PRD was cylindrically symmetric so that the incidence of the simulation only considered the changes of the polar angle. In one process of the simulation, one million of electrons were simulated to input to the head from a source of a circular plane of 5 cm radius in a polar angle. The simulation was completed if the polar angle changed from 0° to 90° since the incidence from the back of the head might be shielded by the satellite body. S_1 and S_2 were used to discriminate the two energy bins and obtain the counts.

The GFs of the two bins were derived from the counts as well as the integration of the polar angles. Assuming the electron radiation isotropic, one has

$$GF = \sum_i \frac{\pi r_0^2 C_i}{N} \delta_i (\mathrm{cm^2 sr}),$$
$$\sum_i \delta_i = 2\pi, \tag{3}$$

where C_i is the number of counts of the second detector in a different incident angle. r_0 is the radius of the source, which is 5 cm and large enough to cover the head. δ_i is the solid angle in a different incident angle. The results show that the GF of the low energy bin for the AE-8 model of the solar minimum and solar maximum are 1.12 and 1.18 $\rm cm^2$ sr, respectively while the GF of the high energy bin for the AE-8 model of the solar minimum and solar maximum are 0.68 and 0.71 $\rm cm^2$ sr, respectively. By averaging the results of the solar minimum and solar maximum, the GF of the

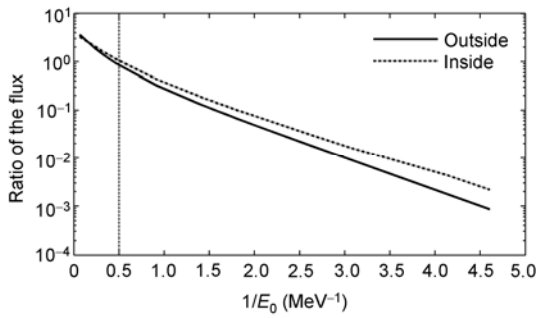

Figure 5 Ratio of the flux of the high energy bin to the flux of low energy bin.

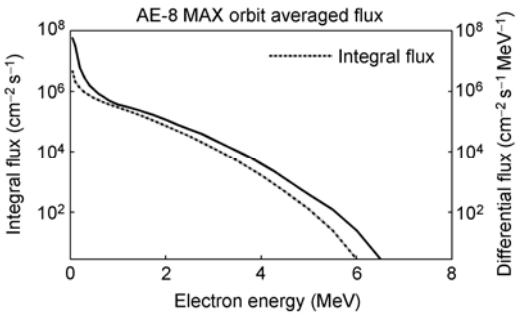

Figure 6 Different and integral fluxes calculated using the AE8-max model.

low and high energy bins are 1.15 and 0.70 cm^2 sr, respectively.

The GF of the low energy bin is larger than that of the high energy bin as Chen et al. suggested. But both of them are smaller than the results of Chen et al. that were 2.468 and 1.736 cm^2 sr for the low and the high energy bins, respectively. It attributes to the scattering and straggle effects of electrons in the matter that Chen et al. did not consider. The scattering and straggle effects of MeV electrons are very strong, and cause the uncertainties of the range of electrons in matter. Part of electrons are shielded by the layers of the light block and the ΔE detector that are both located in the front of the second detector because the real ranges are short due to scattering and straggle effect. These effects decrease the efficiency of the head. Geant4 can precisely simulate the behavior of every step of the electrons in the matter. Therefore, the scattering effect, straggle effect and shielding effects can be fully considered [11].

6 Conclusion

This article investigates the environment of the electron radiation inside the satellite by using the Geant4 simulation about PRD and satellite skin. The corresponding energy bins of PRD outside the satellite are 0.99–2.52 MeV and >2.52 MeV, respectively. They are lower than previous calculated values because the satellite skin was equivalent to one millimeter aluminum rather than two millimeter aluminum. Besides the changes of the energy bins, the fluxes inside are smaller than that of corresponding bins outside. The spectrum inside is harder than that outside. An indicator is that the flux ratio of the high energy bin to the low energy bin increases more than 20% from outside to inside.

The geometric factors of the two bins are determined by using the AE-8 model to derive the incident spectrum. It agrees with the results of Chen el al. in that the GF of the low energy bin is larger than that of the high energy bin. However, the GFs are both smaller than Chen's results. The reason is that Chen el al. did not consider the scattering and straggle effects of electrons, which can shield part of the electrons to the energy detector of the head.

This work was supported by the Special Foundation of China Meteorological Administration (Grant No. GYHY200706041) and the Foundation of Co-construction of Beijing Municipal Commission of Education (Grant No. XK100010404).

1 Xiao Z, Zou J Q, Zou H, et al. Energetic particle detector on board "ZY-1" satellite. Acta Sci Natur Univ Pekin, 2003, 39: 361–369
2 Xiao Z, Zou H, Wu Z, et al. Energetic particle event observed by a polar orbit satellite at 780 km. Acta Sci Natur Univ Pekin, 2003, 39: 370–374
3 Zou H, Xiao Z, Zou J Q, et al. A comparison between detections of energetic electron by ZY1/CBMC and SZ2/XD (in Chinese). Chin J Geophy, 2004, 47: 562–570
4 Zou H, Xiao Z, Hao Y Q, et al. Analysis of the observation of particle detector inside 'CBERS-1' satellite under solar quiet conditions. Sci China Ser E-Tech Sci, 2006, 49: 342–357
5 Zou H, Xiao Z, Hao Y Q, et al. Observation of the disturbed events by the particle detector inside "ZY-1" satellite (in Chinese). Chin J Geophy, 2006, 49: 636–664
6 Zou H, Chen H F, Zou J Q, et al. Comparison between observation of the particle detector inside 'ZY-1' satellite and the model of the radiation belt (in Chinese). Chin J Geophy, 2007, 50: 678–683
7 Hao Y Q, Xiao Z, Zou H, et al. Energetic particle radiations measured by particle detector on board CBERS-1 satellite. Chin Sci Bull, 2007, 52: 665–670
8 Zou H. Study on Energetic Particle Radiation Environment Inside Satellite and in Space. Dissertation of Doctoral Degree. Beijing: Peking University, 2003. 45
9 Chen H F, Shi W H, Zou H, et al. Discussion on the geometric factor in the detection of high energy electrons in geospace. Sci China Ser E-Tech Sci, 2008, 51: 1–9
10 Li X C, Chen H F, Zou H. Shielding analysis of satellite skin to high energy electron radiation (in Chinese). Abstract Book of the 23rd National Symposium on Space Exploration. XiaMen, 2010. 44
11 GEANT4 Collaboration, Geant4: A Simulation Toolkit. SLAC Report SLAC-PUB-9350, 2002
12 Geant4 Home Page. http://geant4.cern.ch/
13 Ma W G. Computational Physics (in Chinese). Beijing: Science Press, 2005. 6
14 Jun S L. Monte Carlo Strategies in Scientific Computing. New York: Springer, 2008. 1–19
15 Yan X J, Chen D. A space energetic electron environment model for spacecraft deep dielectric charging evaluation. Spacecraft Environ Eng, 2008, 25: 120–124
16 Rodgers D J, Hunter K A, Wrenn G L. The FLUMIC electron environment model. Proc 8th SCTC, Huntsville, 2003
17 Ryden K A, Morris P A. Observations of internal charging currents in medium earth orbit. IEEE T Plasm Sci, 2008, 36: 2473–2481
18 SPENVIS Home Page. http://www.spenvis.oma.be/spenvis/